Atmospheric Environment Vol. 24B, No. 2, pp. 227–241, 1990.
Printed in Great Britain.

0957-1272/90 $3.00+0.00

AEROSOLS IN SANTIAGO DE CHILE: A STUDY USING RECEPTOR MODELING WITH X-RAY FLUORESCENCE AND SINGLE PARTICLE ANALYSIS

CARLOS M. ROJAS,* PAULO ARTAXO† and RENÉ VAN GRIEKEN
Department of Chemistry, University of Antwerp (U.I.A.), Universiteitsplein 1, B-2610 Wilrijk-Antwerp, Belgium

(*First received* 1 *June* 1988 *and in final form* 23 *February* 1989)

Abstract—Between 15 January and 26 February 1987, 51 fine and coarse mode aerosol samples were collected at the Universidad de Santiago de Chile Planetarium using a dichotomous sampler. The samples were analyzed by X-ray fluorescence for up to 17 elements (Mg, Al, Si, P, S, K, Ca, Ti, V, Cr, Mn, Fe, Ni, Cu, Zn, Br and Pb). Aerosol particles were individually studied by Electron Probe Microanalysis (EPMA) and Laser Microprobe Mass Analysis (LAMMA). The data set consisting of aerosol elemental concentrations and meteorological variables was subjected to Principal Factor Analysis (PFA), allowing the identification of six fine mode particle source classes (soil, industrial, sulfate particles, traffic, residual oil, wood-burnings), and five coarse mode particle source classes (soil, industrial, traffic, residual oil, sulfate particles). Both PFA solutions explained about 81 and 90% of the total variance in the data set, respectively. The regression of elemental mass concentrations on the Absolute Principal Factor Scores allowed the estimation of the contribution of the different source classes to the Santiago aerosol. Within the fine fraction, secondary SO_4^{2-} particles were responsible for about 49% of the fine mode aerosol mass concentration, while 26, 13, 6.4 and 5.6% were attributed to wood-burning/car exhausts, residual oil combustion, soil dust/metallurgical, and soil dust/wood-burning releases, respectively. The coarse fraction source apportionment was mainly dominated by soil dust, accounting for 74% of the coarse mode aerosol mass concentration. A composite of soil dust and industrial release accounted for 13%; a composite of secondary sulfates contributed with 9%; a composite of soil dust and automotive emissions, and secondary sulfates were responsible for 4 and 0.03% of the coarse aerosol mass concentration, respectively. EPMA results are in satisfactory agreement with those from the bulk analysis and allowed the identification of eight particle types in both fine and coarse mode aerosols, pertaining to different source classes, namely soil, seaspray, secondary SO_4^{2-}, metallurgical emissions and biomass burning release. EPMA also evidenced that one of the most abundant particle types corresponded to marine aerosol, having an average diameter of 0.7 μm for the fine mode and 2.2 μm for the coarse mode aerosol. LAMMA results indicate that, in fact, seaspray has been transported into the city of Santiago de Chile airshed, suffering several transformations and a sulfur enrichment. This analytical technique also provided evidence of the abundance of carbon-rich particles, which were not detected by either the bulk X-ray analysis or EPMA; they are probably due to fossil-fuel combustion releases.

Key word index: Aerosols, receptor models, single particle analysis, source apportionment, X-ray fluorescence, trace metals, dichotomous samplers, elemental composition.

INTRODUCTION

The geographical location and the topographical configuration plus an expanding population involving an increasing rate of anthropogenic emissions of particulate matter make the air pollution in the city of Santiago de Chile severe, and often pollutant levels, particularly sulfur oxides, exceed the international guidelines for exposure limits. To that it has to be added that a thermal inversion layer is present almost all year round and the average rainfall per year is low, which reduces the probability of pollutant removal by washout. Quantitative studies on air pollution in Santiago de Chile only began in the late 1970s, when Rancitelli *et al.* (1977) reported trace elemental concentrations at ground level in several Chilean cities, including Santiago. Silo and Lissi (1982) correlated S concentrations in Santiago with visibility. Préndez *et al.* (1984) measured elemental concentrations in total suspended matter and performed enrichment factor calculations. The first study on inhalable particulate matter (IPM) obtained by dichotomous sampling, was carried out by Trier (1984), who reported coarse/fine concentration correlations for several elements. Trier and Silva (1987) reported seasonal trends of air pollution; also their work constitutes the first attempt to join together dichotomous sampling, elemental analyses and a receptor model such as Principal Component Analysis (PCA), in order to identify the pollution sources affecting the monitoring site. Up to now, detailed information concerning elemental concentrations in IPM obtained by dichotomous sampling was not available for Santiago, and a quantitative assessment of source contributions to particulate matter air pollution was still lacking.

* On leave from: Departamento de Fisica, Universidad de Santiago de Chile.
† Present address: Instituto de Fisica, Universidade de Sao Paulo, Brazil.

In this work, Principal Factor Analysis (PFA) is applied to a data set consisting of both fine and coarse mode aerosol elemental concentrations, including meteorological variables collected over a 2-month period in the city of Santiago de Chile. Based on these PFA results, fine and coarse aerosol pollution sources affecting the monitoring site are identified. The source profiles and the aerosol mass contribution of each identified source is estimated following the absolute principal factor analysis (APFA) procedure described by Thurston and Spengler (1985). The results of the microanalytical techniques have complemented those from bulk X-ray fluorescence (XRF) combined with APFA. Electron probe microanalysis (EPMA) revealed some additional group of elements and laser microprobe mass analysis (LAMMA) allowed the study of the organic constituents of individual particles.

EXPERIMENTAL

Sampling

The 51 fine and coarse IPM samples studied in this work were each collected for 12 h on Teflon membrane filters (2 μm pore-size) during a period spanning from 15 January to 25 February 1987. Fine particles had 50% cut-off diameter at 2.5 μm, while coarse particles corresponded to aerodynamic diameters between 2.5 and 15 μm. The sampler used was a Sierra 244-X dichotomous sampler situated at the Universidad de Santiago de Chile Planetarium, about 4 km west of downtown Santiago, at a height of 10 m above the ground. A schematic map of the sampling site is shown in Fig. 1. Its surroundings are mainly characterized by heavy traffic, a busy thoroughfare, metallurgical activities, and a few industrial wood-burned ovens.

Samples for EPMA were collected for 12 h using a 47 mm diameter stacked filter unit (Parker *et al.*, 1977) operating at flow ranging from 2 to 12 $\ell\,m^{-1}$. Fine and coarse particles were collected on Nuclepore filters, having 0.4 and 8.0 μm pore-size, respectively. The sampling for LAMMA was carried out using a five-stage single-orifice Battelle-type cascade impactor (Bauman *et al.*, 1981) operated at 1 $\ell\,m^{-1}$. The equivalent aerodynamic diameter ranges for the particles collected at the different stages are: >4 μm, 4–2 μm, 2–1 μm, 1–0.5 μm and 0–0.25 μm for stages 1–5, respectively. The aerosol was collected on a 300 mesh electron-microscope grid coated with a thin Formvar film.

Analytical techniques

The samples were analyzed for up to 17 elements (Mg, Al, Si, P, S, K, Ca, Ti, V, Cr, Mn, Fe, Ni, Cu, Zn, Br and Pb) by Energy Dispersive X-ray Fluorescence (XRF) using a X-ray spectrometer Tracor Northern Spectrace 5000 (Tracor Northern, Middleton, WI, U.S.A.), equipped with a Si(Li) detector and a low power X-ray tube with a Rh target, controlled by an IBM PC/AT microcomputer. The calibration of the X-ray spectrometer was performed using thin film standards from Micromatter Co. (Seattle, WA, U.S.A.). The samples were analyzed under two different excitation conditions. For low-Z elements (Mg, Al, Si, P, S), they were irradiated using 35 kV accelerating voltage and 0.02 mA filament current. Elements with atomic number higher than 19 were excited using 35 kV accelerating voltage and 0.35 mA filament current. In order to eliminate part of the Bremsstrahlung continuum, a thin rhodium filter (0.05 mm thick) was placed in front of the X-ray tube window, allowing an improvement of the detection limit, especially for those elements whose spectral lines are slightly above the Rh–L absorption edge. The determination of Na and Cl with this spectrometer was rather difficult since both elements appeared overlapped by Rh–L escape-peaks and Rh–L spectral lines, respectively. The X-ray spectra were accumulated for 5000 s and analyzed using the AXIL software package developed by Van Espen *et al.* (1986). For low-Z elements, absorption and particle size corrections were carried out using the method described by Dzubay and

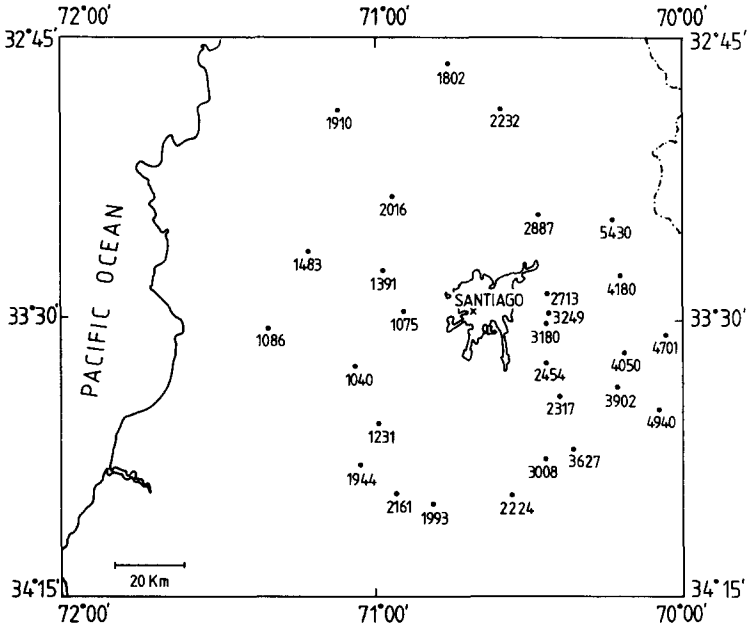

Fig. 1. Schematic representation of the city of Santiago de Chile, containing its geographical coordinates, elevations surrounding the area (in m), and the physical location of the sampling site (X) (extracted from Trier and Silva (1987) *Atmospheric Environment* **21**, 977–984).

Nelson (1975). The collected aerosol mass was determined by simply weighing the Teflon filter before and after sampling using a BOSCH S2000 microbalance, in a controlled atmosphere room.

EPMA analyses were performed using a JXA-733 electron-probe X-ray microanalyzer (JEOL, Tokyo, Japan) equipped with a Tracor Northern TN-2000 energy-dispersive X-ray detection system that allows a fully automatic analysis of a preset number of particles. Morphological information as average diameter and shape factor is provided, whereas compositional data are derived from the X-ray pattern for each particle. Detailed information regarding the EPMA technique can be found elsewhere (Goldstein *et al.*, 1981; Heinrich, 1981; Storms *et al.*, 1987). Samples were analyzed using an electron beam current of 1 nA, an accelerating voltage of 20 kV and a magnification of 1200 X. The measuring time was 20 s for each aerosol particle. Thus 500 particles were analyzed for each sample. The minimum detectable particle size was 0.26 μm.

LAMMA spectra were obtained with the LAMMA-500 instrument of Leybold-Heraeus, Köln, F.R.G. (Vogt *et al.*, 1981; Denoyer *et al.*, 1982), equipped with a Nd-YAG high powered laser. Aerosol particles were vaporized by a single laser pulse ($\tau = 15$ ns), having a wavelength of 265 nm, and a power density in the order of 10^{11} W cm^{-2}. A laser shot converts an aerosol particle into a microplasma which expands towards the entrance of the time-of-flight mass spectrometer. The plasma contains electrically neutral fragments, atomic ions, and molecular ions derived from the constituents of the analyzed particle. LAMMA spectra were stored on an IBM PC/AT microcomputer for off-line analysis.

Receptor models

The various receptor models, either multivariate techniques or chemical mass balance approaches, commonly used in aerosol source identification and apportionment, appear described in detail in the reports of the Quail Roost II workshop (Henry *et al.*, 1984; Dzubay and Stevens, 1984; Stevens and Thompson, 1984). In this work, in order to identify the different sources affecting the monitoring site, Principal Factor Analysis (Hopke *et al.*, 1976; Alpert and Hopke, 1980) was performed with orthogonal VARIMAX rotation and OBLIMIN oblique rotation. The theoretical aspects of factor analysis with oblique rotations are discussed in detail by Rummel (1970) and Gorsuch (1983). In factor analysis it is usually common to come across with orthogonal rotations of the factor loading matrix; however, in practical applications, the factor structure is not orthogonal. If the factors are in fact orthogonal, then an oblique rotation will result in orthogonal dimensions. The results of an oblique rotation consist of factor-pattern and structure matrices and a factor correlation matrix. The pattern matrix is composed of projections (loadings) of a point, which were determined by lines parallel to the factors; whereas the structure matrix contains the projections of a point, measured by lines from the point perpendicular to each factor. The factor matrices allow comparison and interpretation of the oblique factors, whereas the factor correlation matrix contains the pattern of relationship between the factors. Thus, the standardized trace element concentrations can be expressed as a linear combination of the factor loadings, which are correlations between the extracted factors and the variables, and the factor scores, representing the strength of each factor in every sample. Since the factor scores are computed from the standardized variables, they are also standardized, i.e. the source impact has a mean of zero and standard deviation of one. To have a quantitative estimate of the mean source impact, absolute principal factor analysis (APFA) (Thurston and Spengler, 1985), was carried out. The APFA consists mainly of computing the absolute principal factor scores (APFS), where the elemental contribution of each identified source is calculated by regressing the sample elemental concentrations on these APFS.

In order to include, in the data matrix subjected to PFA, the set consisting of 1-h time resolved wind direction measurements obtained at the Santiago de Chile International Airport, it was necessary to reduce them by calculating the average vector corresponding to each sampling period of 12-h. The resulting vectors were transformed into two new variables (NS, EW) following the approach described by Tuncel *et al.* (1985). Here NS and EW indicate wind directions from north–south and east–west, respectively. (NS = +1: north; NS = −1: south; EW = +1: east; EW = −1: west).

RESULTS AND DISCUSSION

Bulk analysis results

The maximum, minimum, average and standard deviation values of the aerosol elemental concentrations obtained for both fine and coarse fractions, are shown in Table 1. Two samples in the fine mode aerosol and three samples in the coarse mode aerosol had very high concentrations and therefore were excluded from the study, classified as outliers due to their episodic nature. Elements which were not present above the detection limit in all samples of a size fraction were excluded from the statistical analysis, namely, Mg, Ca, Ti, Cr and Ni in the fine fraction, and Cr and Ni in the coarse fraction. Values in parentheses indicate the number of samples in which the element exceeded the detection limit defined by 3 times the standard deviation of the concentration measurement. We can notice in this table the relatively high concentration of S in the fine mode aerosol, while the coarse mode aerosol appears dominated by soil related elements. In general, both fine and coarse elemental concentrations are lower than those reported previously by Rancitelli *et al.* (1977). However, similarities were observed for Br and Cr. The average Br/Pb ratio (0.20) is lower than that reported in the literature for fresh car exhausts (0.39) by Harrison and Sturges (1983), and for average automotive emission (0.45) as listed in the Receptor Model Source Composition Library (RMSCL) (1984). However, this ratio is similar to that (0.20) reported by Öblad and Selin (1985), when a background lead concentration is present. Therefore, it is thought that in our case, automotive emissions do not constitute the only source of atmospheric Pb.

Based on the average elemental concentrations, enrichment factors (EF) relative to the earth's crust (Mason, 1966), are presented in Table 2. In general, the EF calculation appears related to subjective basis and the researcher's choice on which element is the most suitable for normalization purposes, does not follow a strict rule. In this work we have chosen Al as reference element in order to compare our results with those corresponding to 29 different urban areas, determined using the same element and reported by Rahn (1976). It is seen that there are well-marked differences from fraction to fraction and only the EFs of Mg, Si, Ca, Ti

Table 1. Average Santiago de Chile fine and coarse elemental and mass concentrations. The numbers in parentheses indicate the number of samples in which the element has been measured above the detection limit

		Concentrations ($ng\,m^{-3}$) Fine fraction				Coarse fraction		
Element		Aver. ± s.d.	Min	Max		Aver. ± s.d.	Min	Max
Mg	(12)	40 ± 20	11	80	(48)	250 ± 100	70	440
Al	(49)	180 ± 70	60	390	(48)	1960 ± 710	810	3400
Si	(49)	660 ± 350	200	2080	(48)	5400 ± 1970	2080	9300
P	(49)	90 ± 40	30	180	(48)	90 ± 20	50	130
S	(49)	2100 ± 1080	650	4450	(48)	420 ± 150	170	730
K	(49)	980 ± 460	460	2200	(48)	960 ± 330	480	1710
Ca	(28)	280 ± 70	110	390	(48)	2720 ± 950	1240	5040
Ti	(4)	17 ± 2	15	20	(48)	260 ± 100	90	490
V	(49)	16 ± 8	5	40	(48)	11 ± 5	4	21.2
Cr	(4)	6.5 ± 2.1	3.7	8.4	(4)	15 ± 5	12	23
Mn	(49)	17 ± 11	6	50	(48)	80 ± 30	40	140
Fe	(49)	200 ± 90	70	450	(48)	2930 ± 1100	1180	5430
Ni	(22)	3.3 ± 0.9	2.3	5.4	(27)	2.5 ± 2.4	0.2	10
Cu	(49)	26 ± 16	9	80	(48)	40 ± 20	20	80
Zn	(49)	220 ± 180	26	790	(48)	90 ± 50	30	230
Br	(49)	50 ± 20	26	110	(48)	21 ± 6	13	41
Pb	(49)	260 ± 120	120	590	(48)	100 ± 30	50	200
Mass	(49)	34,000 ± 13,000	15,000	61,000	(48)	66,000 ± 24,000	36,000	125,000

Table 2. Enrichment factors relative to the earth's crust based on elemental concentrations and determined with respect to Al (see text)

	Enrichment factor		
Element	Fine fraction	Coarse fraction	Geometric mean from 29 cities*
Mg	0.9	0.5	2.0
Al	1.0	1.0	1.0
Si	1.1	0.8	0.8
P	51	5.0	2.6
S	3920	70	490
K	17	1.5	1.6
Ca	2.6	3.1	2.9
Ti	2.0	2.6	1.6
V	45	3.0	15
Cr	32	6.2	6.2
Mn	9.0	4.0	3.2
Fe	1.8	2.4	2.2
Ni	18	1.0	11
Cu	140	29	150
Zn	1200	56	300
Br	9300	325	1940
Pb	9100	313	3800

* Rahn (1976).

remain more or less unaltered. This is consistent with results reported by Schütz and Rahn (1982), who found that the elemental composition of erodible soils remained fairly constant in the size range between 1 and 20 μm diameter. Furthermore, their EFs are comparable to the mean values corresponding to other sites. The fine fraction presents high enrichments for P, S, K, V, Mn, Ni, Cu, Zn, Br and Pb. However, in the coarse fraction K and Ni have an EF-value which suggests that they are most likely soil related. In the fine fraction their enrichment could be due to biomass burning (for K) and residual oil combustion (for Ni). The elements having a moderate EF in the coarse aerosol mode are: P, Cr, Mn; while S, Cu, Zn, Br and Pb appear highly enriched.

Principal Factor Analysis of the fine mode aerosol

The PFA on the 15 variables (Al, Si, P, S, K, V, Mn, Fe, Cu, Zn, Br, Pb, fine particles mass concentration, NS and EW) yielded four eigenvalues >1, while the fifth and sixth had values of 0.9 and 0.7, respectively. Since there is no standard procedure of choosing the number of factors to be retained, the following step consisted of rotating the resulting factor matrix when four, five and six factors were retained, each time. The VARIMAX rotated matrices were thoroughly compared and analyzed. The four-factor solution had low communalities for most of the variables and the factor identification was rather difficult. On the other hand, the six-factor solution led to the same conclusions as when five factors were retained, with the only difference that the variable representing east–west wind directions appeared isolated in the sixth factor. Hence, the source identification discussed below has been based on the five-factor solution.

Results of the VARIMAX rotated factor analysis on the fine mode elemental concentration data with fine particles mass concentration and wind direction patterns, are shown in Table 3. In this table only those factor loadings exceeding 3 times their standard deviation (Heidam, 1982) are shown, together with the communality for each variable, and the eigenvalues obtained after rotation.

The five-factor solution accounts for 81% of the total variance and the communalities are relatively high for all variables, with the exception of the wind

Table 3. VARIMAX rotated factor loading matrix for the Principal Factor Analysis of 49 fine mode aerosol samples from Santiago de Chile. Factor loadings greater than 3 times their standard deviation are shown

Variable	Factor 1	Factor 2	Factor 3	Factor 4	Factor 5	Communality
Al	0.84	–	–	–	–	0.82
Si	0.79	–	–	–	–	0.76
P	0.33	0.87	–	–	–	0.89
S	–	0.91	−0.23	–	–	0.92
K	–	–	–	–	0.93	0.92
V	–	–	0.50	−0.48	0.55	0.81
Mn	0.81	–	0.28	–	–	0.82
Fe	0.88	–	0.25	–	–	0.86
Cu	0.85	–	–	–	–	0.78
Zn	0.83	0.26	0.28	–	–	0.86
Br	–	–	0.79	–	–	0.77
Pb	0.61	0.39	0.43	0.33	–	0.83
Mass	–	0.73	–	–	0.33	0.77
NS	–	–	–	0.89	–	0.80
EW	–	0.56	–	–	–	0.49
Eigenvalue	4.9	2.8	1.5	1.5	1.5	
% variance explained	32.7	18.7	10.0	10.0	10.0	
Possible identif.	Soil dust/ industrial	Sulfate	Automotive emissions	North wind	Wood-burning	

EW variable. Factor 1 had high loadings for Al, Si, P, Mn, Fe, Cu, Zn and Pb; which probably indicates a composite of soil related aerosol with an industrial source (foundries, metallurgical activities). This factor does not appear related to any specific wind direction. Factor 2 consisted of high loadings for S, P and mass. It is suggested that this factor represents secondary sulfates; the presence of P in this factor can with difficulty be ascribed to any source. The east component of the wind direction has a moderate loading in this factor, while Zn, Pb had low loadings. Factor 3 had a high loading for Br, moderate loadings for V, Pb, and low loadings for Mn, Fe, Zn. It seems that this factor is associated with car exhaust since Br and Pb are attributed to leaded fuel combustion (Cooper and Watson, 1980). On the other hand, V is probably linked to oil combustion processes. Factor 4 had high loading for the north component of the wind direction. There is a moderate but negative loading for V in this factor which suggests that, when wind blows from the north, the source emitting V (probably oil combustion) has less impact on the monitoring site. In factor 5 we find a high loading for K and a moderate loading for V. The presence of K is possibly related to wood-burning, since in the neighborhood of the sampling site, there are a number of bakeries equipped with wood-fired ovens. On the other hand, during the dry season (December–February) there is plenty of wild forest fires and agricultural field burning which might have their impact on the sampling site. The loading for V could be due to residual oil combustion.

In summary, the results of the PFA of the fine mode aerosol indicate that for the 15 measured variables, six classes of aerosol sources can be distinguished: soil dust aerosol (for Al, Si, Fe), metallurgical processes (for Mn, Cu, Zn), secondary sulfates (for S), wood-burning (for K), automotive emissions (for Br, Pb), and residual oil combustion (for V). It was not possible to ascribe a source for P. Pb is possibly originating from metallurgical activities and also from automotive emissions. On the other hand, fine particle mass appeared associated mainly with secondary SO_4^{2-}, with a low loading for wood-burning.

Principal Factor Analysis of the coarse mode aerosol

The PFA on the 18 variables (Mg, Al, Si, P, S, K, Ca, Ti, V, Mn, Fe, Cu, Zn, Br, Pb, mass concentration, NS, EW), forming part of the coarse mode data set had a solution consisting of four eigenvalues >1, while the fifth and sixth had values of 0.8 and 0.6, respectively. As for the fine mode analysis, when four factors were retained the communalities were low and the source identification was rather difficult. On the other hand, no significant changes in the source compositions were observed when six factors were retained instead. Therefore, the VARIMAX rotated PFA for coarse mode elemental concentrations, mass concentration and wind direction patterns presented in Table 4 consists of five factors accounting for 91% of the total variance in the data set. The communality presents high values for most of the variables. In this case, 68% of the total variance is accounted for by the first two factors.

Factor 1 had high loadings for Mg, Al, Si, P, K, Ca, Ti, Mn, Fe and mass; it can be ascribed to soil dust with some industrial contribution. The N component of the wind direction, and also Cu, present a moderate loading. Factor 2 has high loadings for V, Cu, Zn and Pb, and it is related to industrial activities and residual oil combustion. Mn has a moderate loading in this second factor. No specific wind direction trend is

Table 4. VARIMAX rotated factor loading matrix for the Principal Factor Analysis of 48 coarse mode aerosol samples from Santiago de Chile. Factor loadings greater than 3 times their standard deviation are listed

Variable	Factor 1	Factor 2	Factor 3	Factor 4	Factor 5	Communality
Mg	0.93	–	–	–	–	0.93
Al	0.97	–	–	–	–	0.98
Si	0.97	–	–	–	–	0.98
P	0.83	–	0.26	–	–	0.89
S	–	–	–	–	0.93	0.91
K	0.97	–	–	–	–	0.99
Ca	0.94	–	–	–	–	0.97
Ti	0.97	–	–	–	–	0.98
V	–	0.75	–	–	–	0.74
Mn	0.89	0.40	–	–	–	0.95
Fe	0.97	–	–	–	–	0.99
Cu	0.62	0.64	–	–	–	0.87
Zn	0.31	0.78	–	–	–	0.79
Br	–	–	0.92	–	–	0.88
Pb	0.30	0.68	0.54	–	–	0.88
Mass	0.88	0.27	–	–	–	0.90
NS	0.43	–	–	0.51	–	0.68
EW	–	–	–	0.91	–	0.88
Eigenvalue	9.6	2.7	1.4	1.3	1.3	
% variance explained	53.3	15.0	7.8	7.2	7.2	
Possible identif.	Soil dust	Oil/ industrial	Automotive emissions	EW wind	Secondary sulfates	

observable. Factor 3 consisted of high loadings for Br and Pb; this factor presumably represents automotive emissions, since both Br and Pb are tracers for leaded fuel combustion. This factor has also a low loading for P, and similarly to the fine fraction, the presence of P cannot be ascribed to any source in particular. Factor 4 had a high loading for the east component of the wind direction, and a moderate loading for the north component. This factor is likely to represent only meteorological variations relative to wind direction. Factor 5 shows high loading for sulphur. The loadings for the south component of the wind and the mass, are also noticeable in this factor, that represents sulfates.

The PFA of the coarse mode aerosol elemental concentrations has discriminated five different sources. These were: soil dust (for Mg, Al, Si, K, Ca, Ti, Fe), industrial sources (for Mn, Cu, Zn), traffic (for Br), sulfates (for S), and residual oil combustion (for V). The presence of Zn and Pb in factor 1 might indicate that car exhaust is not the only source of Pb. The coarse mode mass concentration appeared associated with soil dust and industrial emissions.

The source identification for both aerosol modes above discussed has been based on the assumption that factors were orthogonal. Since sources seem slightly mixed up, one could draw the conclusion that an oblique rotation of the factors might lead to a better resolution of the sources impacting our sampling site. An oblique rotation such as OBLIMIN was performed and the results are shown in Tables 5 and 6 for the fine and coarse mode aerosols, respectively. Within the fine mode one can observe that there are not well marked differences between pattern and structure matrices, suggesting that factors are most likely orthogonal. This fact appears sustained by the low correlations observed in the factor correlation matrix, indicating that there is a weak relationship between the factors. The OBLIMIN factor rotated solution for the coarse mode aerosol data set shows that both pattern and structure matrices have high loadings for factor 1, particularly for the soil related elements; however, these elements have also significant loadings in the second factor (see structure matrix). For the rest of the factors, both matrices present comparable loadings. The correlation between factor 1 and 2 (0.48) suggests that these two factors have soil-related elements in common, and that this aerosol has been long enough in the atmosphere to be able to interact with industrial emissions. Since the oblique rotated factor solutions do not essentially differ from the original VARIMAX rotated solutions, and do not provide any substantial improvement in the source indentification, orthogonal rotations will be used in the following sections.

Absolute Principal Factor Analysis of fine mode aerosol

In order to derive the source profiles, the elemental concentrations were subjected to multiple linear regression on the APFS, and each regression coefficient was checked to determine its statistical significance level and validity. The source profiles of the fine mode aerosol are shown in Table 7 and Fig. 2, respectively. It is seen that the first component contains a composite of soil dust, SO_4^{2-} particles, industrial emissions, and

Table 5. OBLIMIN (oblique) factor rotated solution of the Santiago fine mode aerosol. Factor analysis consisting of pattern matrix, structure matrix and the factor correlation matrix

Pattern matrix					
Variable	Factor 1	Factor 2	Factor 3	Factor 4	Factor 5
Al	0.83	–	–	–	–
Si	0.79	–	–	–	–
P	–	0.87	–	–	–
S	–	0.92	–	–	–
K	–	–	–	–	0.97
V	–	–	0.41	−0.40	0.52
Mn	0.81	–	–	–	–
Fe	0.87	–	–	–	–
Cu	0.87	–	–	–	–
Zn	0.84	–	–	–	–
Br	–	–	0.77	–	–
Pb	0.58	0.30	0.41	0.33	–
Mass	–	0.74	–	–	0.30
NS	–	–	–	0.90	–
EW	–	0.55	–	0.30	–
Structure matrix					
Variable	Factor 1	Factor 2	Factor 3	Factor 4	Factor 5
Al	0.84	–	–	–	–
Si	0.77	–	–	–	–
P	–	0.89	–	–	–
S	–	0.92	–	–	–
K	–	–	–	–	0.94
V	–	–	0.54	−0.55	0.67
Mn	0.85	–	–	–	–
Fe	0.91	–	–	–	–
Cu	0.87	–	–	–	–
Zn	0.86	–	–	–	–
Br	–	–	0.80	–	–
Pb	0.67	0.43	0.46	0.35	–
Mass	–	0.72	–	–	0.34
NS	–	–	–	0.89	–
EW	–	0.55	–	–	–
Factor correlation matrix					
	Factor 1	Factor 2	Factor 3	Factor 4	Factor 5
Factor 1	1.00				
Factor 2	0.14	1.00			
Factor 3	0.16	0.07	1.00		
Factor 4	0.04	0.06	−0.12	1.00	
Factor 5	0.21	−0.05	0.14	−0.19	1.00

car exhausts. The first factor contributes most to the measured fine mode concentrations of Mn, Fe, Cu, Zn and Pb by 65, 47, 62, 82 and 45%, respectively. Because of its elemental profile, this factor can be associated with metallurgical emissions. The second component is mainly characterized by S, probably from secondary SO_4^{2-}, accounting for *ca* 98% of the measured S concentration. The third component mainly consists of K, most likely from wood-burning release, containing about 63 and 63% of the total K and V concentration, respectively. It also contains Br and Pb which are associated with automotive emissions. The fourth component suggests the presence of a composite of soil dust and wood-burning release, with Si and K being the most noticeable contributions. From the regression coefficients, the mass contribution of this factor was statistically insignificant. The value tabulated with an asterisk was computed taking Si and K as tracers, and the average soil and wood-burning source profiles extracted from the RMSCL (1984). Even though this procedure of calculating the mass apportionment contains a great deal of error, the resulting value does not considerably affect the total mass contribution accounted for by the remaining factors. The fifth component contributes mainly with V, Mn and Fe. V is associated with residual oil combustion processes, while Mn and Fe are probably released from metallurgical activities. The Br/Pb ratio in the first component (0.10) indicates that there is a possible industrial source of Pb, whereas the ratio obtained in the third component (0.51) is similar to that reported by the RMSCL (1984), regarding automotive emissions (0.45).

Absolute Principal Factor Analysis of coarse mode aerosol

The source profiles of the coarse mode aerosol, shown in Table 8 and Fig. 2 present a similar source

Table 6. OBLIMIN (oblique) factor rotated solution of the Santiago coarse mode aerosol. Factor analysis consisting of pattern matrix, structure matrix and factor correlation matrix

Pattern matrix

Element	Factor 1	Factor 2	Factor 3	Factor 4	Factor 5
Mg	0.94	–	–	–	–
Al	1.00	–	–	–	–
Si	1.00	–	–	–	–
P	0.84	–	–	–	–
S	–	–	–	–	0.94
K	1.00	–	–	–	–
Ca	0.97	–	–	–	–
Ti	1.01	–	–	–	–
V	–	0.79	–	–	–
Mn	0.84	–	–	–	–
Fe	1.00	–	–	–	–
Cu	0.43	0.63	–	–	–
Zn	–	0.78	–	–	–
Br	–	–	–	0.93	–
Pb	–	0.63	–	0.49	–
Mass	0.90	–	–	–	–
NS	0.40	–	0.49	–	−0.37
EW	–	–	0.93	–	–

Structure matrix

Element	Factor 1	Factor 2	Factor 3	Factor 4	Factor 5
Mg	0.96	0.47	–	–	–
Al	0.98	0.43	–	–	–
Si	0.99	0.44	–	–	–
P	0.89	0.55	–	–	–
S	–	–	–	–	0.93
K	0.99	0.48	–	–	–
Ca	0.97	0.50	–	–	–
Ti	0.99	0.45	–	–	–
V	–	0.81	–	–	–
Mn	0.95	0.65	–	–	–
Fe	0.99	0.48	–	–	–
Cu	0.73	0.76	–	–	–
Zn	0.47	0.86	–	–	–
Br	–	–	–	0.93	–
Pb	0.48	0.79	–	0.65	–
Mass	0.93	0.54	–	–	–
NS	0.43	–	0.56	–	−0.43
EW	–	–	0.89	–	–

Factor correlation matrix

	Factor 1	Factor 2	Factor 3	Factor 4	Factor 5
Factor 1	1.00				
Factor 2	0.48	1.00			
Factor 3	0.13	−0.05	1.00		
Factor 4	0.19	0.23	−0.03	1.00	
Factor 5	0.01	0.24	−0.05	−0.03	1.00

composition as in the fine mode. In general the soil component appears more often and the source contribution to S, K, Zn, Br and Pb mass concentrations is much lower than in the fine fraction. The first component consists mainly of soil dust, and it accounts for 73% of the coarse particles mass concentration. The second component contains crustal elements and its contribution to Zn and Pb concentrations represents 31 and 20% of the average concentration for these two elements, respectively. The apportioning of the third component to the S concentration represents about 81% of the total measured S; this probably indicates secondary sulfate particles. The fourth component contains crustal elements together with Br and Pb, accounting for about 76 and 43% of the Br and Pb concentrations. This might indicate soil dust and automotive emissions. Source five consists of S, most likely from secondary sulfates. In this fraction, factor 4 and 5 had a mass contribution statistically insignificant. The mass apportionment of factor 4 was then estimated using Si and Pb as tracers, and the soil and automotive emission source profiles extracted from RMSCL. The mass contribution of factor 5 was calculated as if it was ammonium sulfate. The contribution of the two factors to the measured mass concentration is less than 5%.

Table 7. Source profiles of the Santiago de Chile fine mode aerosol, obtained using APFA. The number in parentheses represents the average measured elemental concentration (in ng m^{-3}). Mass is in $\mu g\, m^{-3}$

Element		Factor 1	Factor 2	Factor 3	Factor 4	Factor 5
Al	(180)	60±5	18±8	34±8	60±5	–
Si	(660)	250±28	83±22	–	290±26	–
P	(93)	14±2	69±3	–	9±2	–
S	(2100)	230±49	2050±74	–	120±46	–
K	(980)	–	130±51	622±50	216±31	–
V	(16)	1.8±0.6	–	10±2	–	5.9±0.8
Mn	(17)	11±2	–	2.6±1.2	–	2.7±1.2
Fe	(200)	94±6	–	44±8	29±5	17±7
Cu	(26)	16±2	5±2	–	3.9±1.2	–
Zn	(220)	180±12	42±18	–	–	–
Br	(50)	12±2	–	35±3	–	–
Pb	(260)	116±11	107±16	67±16	–	–
Mass	(34)	2.4±1.0	18.5±1.7	9.7±1.6	2.1*	4.9±1.5
Possible identif.		Soil dust/ industrial	Secondary sulfates	Wood-burning/ automotive emissions	Soil dust/ wood-burning	Residual oil

* Estimated value (see text).

While the Santiago fine mode aerosol was mainly dominated by S and K containing aerosol, followed by soil dust and industrial emissions, the coarse fraction consists mainly of soil dust associated with industrial release. Sulfur containing aerosol is also noticeable in this fraction. The pie chart shown in Fig. 3a indicates that 49% of the total Santiago fine mode aerosol is attributed to sulfate particles, while 26% comes from wood-burning plus automotive releases. Residual oil combustion processes contribute with 13%, whereas the composites soil dust/industrial and soil dust/ wood-burning represent 6.4 and 5.6% of the total fine fraction, respectively. Figure 3b shows the total mass apportionment of the Santiago coarse mode aerosol, which appears to be 74% due to soil dust, followed by 12.8% coming from a soil dust/industrial composite. The apportioning of a SO_4^{2-} composite is much lower than that of the fine fraction, and represents only 9% of the total coarse fraction aerosol. Soil dust plus automotive emissions contribute with 4% while the remaining (0.02%) has been attributed to SO_4^{2-} particles.

Electron probe microanalysis results

The abundances of the different particle types were determined by a hierarchical (Ward, 1963; Storms, 1988), and non-hierarchical (Anderberg, 1973) cluster analysis. In general, cluster analysis consists of determining the interrelationship of several groups containing interrelated variables. Clustering techniques usually group variables on some measure of relationship between variables, such as correlation coefficient or distance coefficient. In practice, the clustering was performed on the normalized X-ray intensities emitted by each aerosol particle, using the software package (DPP) developed by Van Espen (1984). The study of 2500 particles in each aerosol mode resulted in a matrix containing morphological data as well as elemental composition. The results obtained from analyzing the fine mode aerosol are summarized in Table 9. The number percentage of each particle type is listed, as well as its average diameter, the major elemental X-ray intensities and the possible identification. It is seen that in the fine mode, eight different particle types can be identified based on the major elemental composition. In fact, the most abundant particle type corresponds to soil dust, while the following features marine aerosol. Sulfate, aluminosilicate and metallurgical particles were grouped in 3rd, 4th and 5th place, representing 15, 12 and 10% of the total analyzed particles, respectively. Particle type 6 and 8 could be identified as gypsum and wood-burning release, respectively, whereas particle type 7 features Si–Fe rich particles. These groups were less abundant and they accounted for 9, 4 and 3% of the total. In addition, EPMA on this aerosol mode revealed two natural particle sources, namely, soil dust and marine aerosol, while an anthropogenic source occupied the third place. The particles associated with seaspray, SO_4^{2-}, metallurgical emissions and wood-burning processes had sub-μm diameters, whereas those related to the earth's crust ranged from 1 to 1.6 μm diameter. The apparent contradiction of these results with those from the bulk analysis in which S appears to be the most abundant element in this fraction, can be explained assuming that S-bearing particles had aerodynamic diameters <0.26 μm and, therefore, they were below the minimum detectable particle size. However, six groups out of eight had S forming part of the major elemental X-ray lines, which is a clear evidence of its abundance.

The clustering results for the coarse fraction are shown in Table 10. Within the eight groups observed, it is seen that the most dominating particle type corresponds to soil dust, representing about 60% of the total. The presence of marine aerosol (11%) is also noticeable in this aerosol mode. Particle type 3 had no detectable elements with atomic number higher than

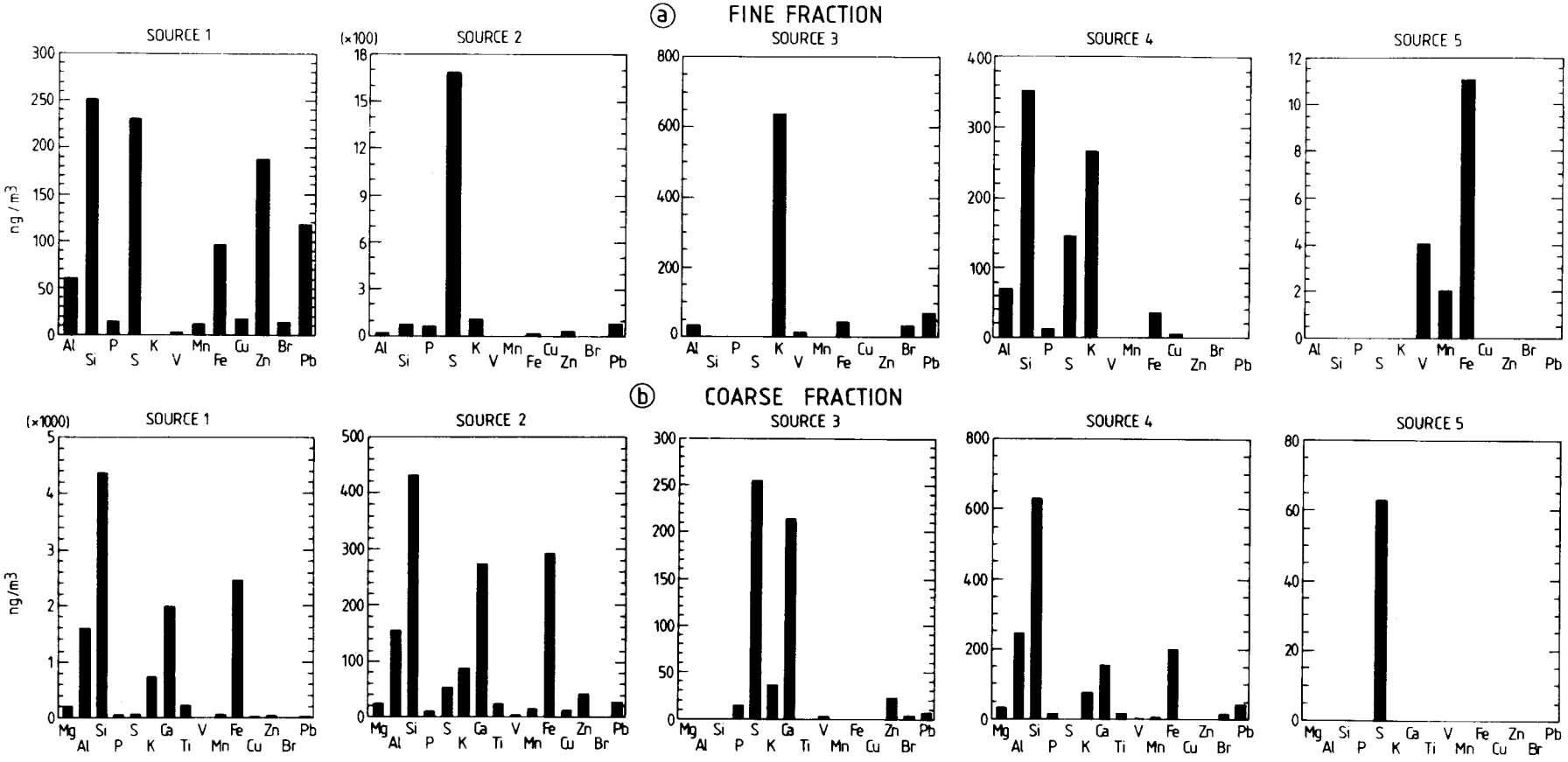

Fig. 2. Fine (a) and coarse (b) aerosol fraction source composition affecting the monitoring site. The ordinate axis represents concentration in ng m^{-3}, while the abscissa axis contains the different elements detected.

Table 8. Source profiles of the Santiago de Chile coarse mode aerosol, obtained using APFA. The number in parentheses stands for the average elemental concentration (in ng m^{-3}). Mass is in μg m^{-3}

Element		Factor 1	Factor 2	Factor 3	Factor 4	Factor 5
Mg	(250)	209±7	17±3	–	33±8	–
Al	(1960)	1630±32	108±13	–	254±35	–
Si	(5400)	4440±71	306±28	–	649±77	–
P	(89)	46±2	6.5±0.9	20±3	16±3	–
S	(420)	54±16	37±9	340±30	–	3.7±1.2
K	(960)	750±9	62±4	49±11	77±10	–
Ca	(2720)	2030±55	190±22	290±69	160±60	–
Ti	(260)	230±4	16±2	–	15±5	–
V	(11)	3.1±0.6	2.2±0.2	2.2±0.8	2.8±0.7	–
Mn	(80)	60±2	9.7±0.7	–	6.2±2.0	–
Fe	(2930)	2520±32	207±12	–	208±34	–
Cu	(40)	27±2	8.8±0.9	–	–	0.4±0.1
Zn	(93)	34±6	29±2	30±8	–	–
Br	(21)	2.4±0.4	1.0±0.2	2.1±0.5	16±1	–
Pb	(100)	27±4	20±1	10±4	43±4	–
Mass	(66)	48±2	5.8±0.9	8.3±2.9	2.6*	0.02*
Possible identif.		Soil dust	Soil dust/ industrial	Sulfates composite	Soil dust/ automotive emissions	Secondary sulfate

* Estimated value (see text).

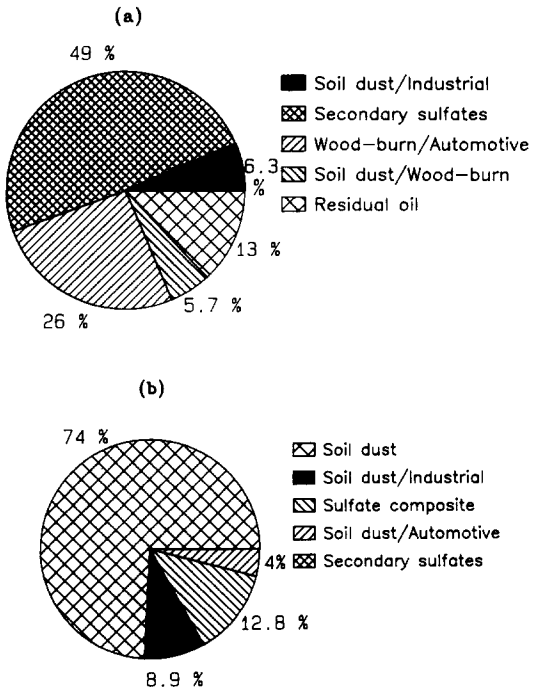

Fig. 3. Fine (a) and coarse (b) mass concentration source apportionments for the Santiago de Chile aerosol.

10; therefore, it was classified as organic material. Manual electron microscope inspection of some of these particles showed a morphology indicative of biogenic particles (Artaxo *et al.*, 1988), e.g. plant parts. The per cent abundance of this particle type was 8%. Group 4 contained Ca–Si rich particles, representing 7% of the abundance, while groups 5, 6, 7 and 8 presented the same elemental composition as those in the fine mode, characterizing metallurgical, gypsum, Si–Fe rich and wood-burning release particles, respectively. In summary, this fraction is mostly dominated by soil dust as a particulate matter source, followed by marine aerosol, organic material, and some industrial emissions. Those particles associated with anthropogenic activities, namely, SO_4^{2-} and metallurgical emissions, appeared less frequently, and those originated from biomass burning were less abundant. Average particle diameter ranged between 1.4 and 4.2 μm.

The results of EPMA pointed towards the presence of marine aerosol forming part of the Santiago de Chile atmospheric particulate matter and this was rather unexpected. In fact, Préndez *et al.* (1984) reported that the city of Santiago had non-marine impact mainly due its topographical configuration and geographical location. This assumption was based on enrichment factor calculations performed on total suspended matter elemental concentrations.

Laser microprobe mass analysis results

The typical positive ion mode spectrum obtained when analyzing aerosol particles, having aerodynamic diameters corresponding to the fifth stage of the cascade impactor (between 0.25 and 0.5 μm), is shown in Fig. 4a, while the spectrum corresponding to the negative ion mode appears in Fig. 4b. The positive spectrum is mainly characterized by Na and several molecular fragments containing this element. This spectrum, in fact, corresponds to a transformed seasalt particle still containing remains of its original NaCl content located at 81 amu. There is also a S-enrichment present in most of the spectra pertaining to this type of aerosol particles. This has been previously reported by Andreae *et al.* (1986) and Clegg

Table 9. EPMA results of the Santiago fine mode aerosol

Particle type number	Abundance (%)	Average diameter (μm)	Major elemental* X-ray intensities	Possible source
1	28	1.6	Si, Ca, Fe, Al	Soil dust
2	19	0.7	Cl, S, K, Na	Seaspray
3	15	0.7	S, Cu, Pb	Sulfate aerosol
4	12	1.2	Al, Si	Aluminosilicate
5	10	0.6	S, Cu, Zn, Pb	Metallurgical
6	9	1.2	Ca, S	Gypsum
7	4	1.0	Si, Fe, S	Si–Fe rich
8	3	0.6	K, Cl, S	Biomass burning

* The order in which elements are placed indicates the intensity of the X-ray lines.

Table 10. EPMA results of the Santiago coarse mode aerosol

Particle type number	Abundance (%)	Average diameter (μm)	Major elemental* X-ray intensities	Possible source
1	58	3.8	Si, Ca, Fe, Al	Soil dust
2	11	2.2	Cl, Na	Seaspray
3	8	3.0	none	Organic
4	7	3.6	Ca, Si	Ca–Si rich
5	6	1.4	S, Cu, Zn	Metallurgical
6	6	2.6	Ca, S	Gypsum
7	3	2.8	Si, Fe	Si–Fe rich
8	1	4.2	Cl, K	Biomass burning

* The order in which elements are placed indicates the intensity of the X-ray lines.

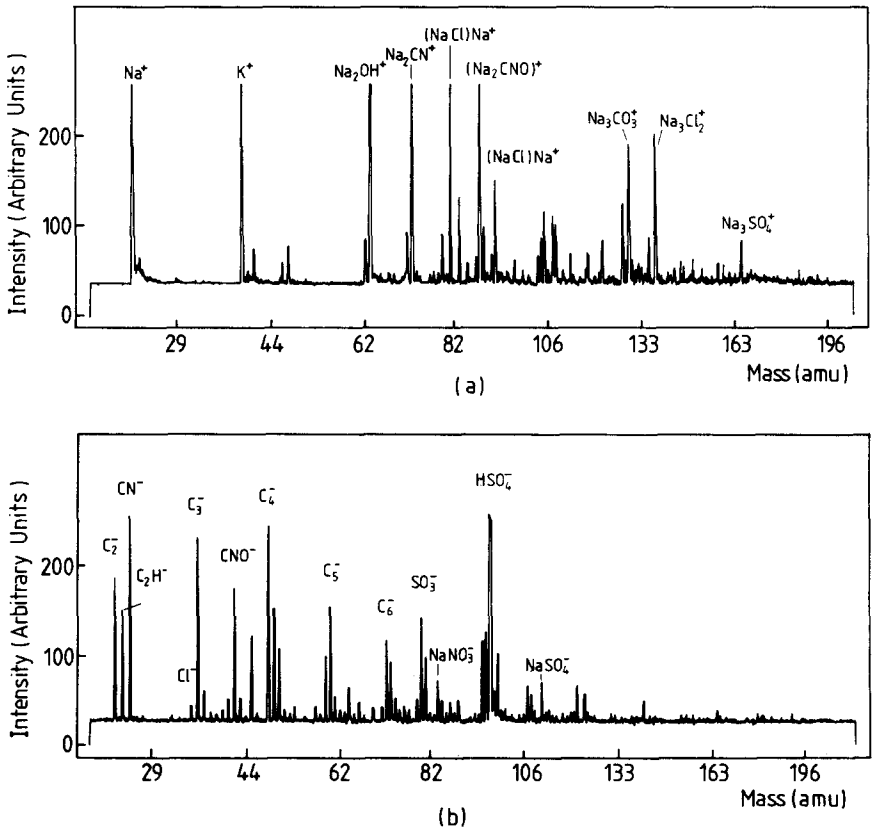

Fig. 4. Positive (a) and negative (b) ion mass spectra corresponding to a transformed seasalt particle with an average diameter ranging from 0.25 to 0.50 μm.

and Brimblecombe (1985) regarding the mechanism of SO_4^{2-} enrichment of seasalt particles. The K-enrichment, also observed at this size fraction, appears to be in agreement with the previous results and points towards the presence of a K source, probably a wood-burning release. The negative ion mode spectrum shows an enrichment of S together with organic species. In general, the positive ion mode spectrum consisted of different species depending on the particle size fractionation. Thus the spectrum corresponding to particles collected on the first two stages (between 4 and 2 μm aerodynamic diameter) was mainly characterized by Al^+, Si^+, SiO^+, Si_2O^+, $Si_2O_2^+$, Ti^+ and TiO^+, probably associated with large clay minerals. The LAMMA spectra of particles collected on stage three (1.0 μm) often contained Na^+, Ca^+, CaO^+ and $CaOH^+$ and with a relative low frequency Al^+ and K^+. The positive ion pattern of particles collected on stages four and five (0.5 and 0.25 μm) was featured by NH_4^+, Na^+, Na_2OH^+, $Na_3SO_4^+$, $NaKSO_4^+$, Na_2Cl^+, Na_2CN^+, Na_2CNO^+, $NaCO_3^+$, $Na_3Cl_2^+$ and Pb^+. With relatively low abundance, the spectrum contained Mg^+, Al^+, K^+, Ca^+, V^+, Mn^+, Fe^+, Cu^+, Zn^+, $K(CaO)^+$, K_2Cl^+, $K_2SO_4H^+$ and $K_3SO_4^+$. Species containing Na, Cl and S were most abundant on the fifth stage. This is, in fact, evidence that marine aerosol has been transported into the city of Santiago, suffering a S-enrichment generated by anthropogenic sources. The negative ion mode had abundant sulfates, nitrates and in many cases it was uniquely composed of the carbon series. The latter can be attributed to oil combustion release. With relative low frequency, phosphates formed part of the LAMMA negative spectra. The presence of transformed NaCl particles indicates that, in fact, sea aerosol particles have been transported into the Santiago de Chile airshed, which is in agreement with the results obtained by EPMA.

SUMMARY AND CONCLUSIONS

The PFA on the fine mode elemental concentration data yielded to a five-factor solution accounting for about 81% of the total variance, and based on the factor loading matrix, six different pollution sources affecting the monitoring site were identified, namely soil dust, secondary SO_4^{2-}, metallurgical processes, car exhausts, fossil-fuel combustion, and wood-burning release. On the other hand, PFA on the coarse elemental concentration data allowed the identification of five airborne particulate matter sources. These are: soil dust, metallurgical processes, automotive emissions, residual oil combustion and secondary SO_4^{2-}. This solution accounted for about 91% of the total variance in the data set. In both fine and coarse fraction PFA solution, Pb appeared associated with automotive emissions and metallurgical activities.

The orthogonality of the factors was checked by performing an oblique rotation such as OBLIMIN. The results indicated that for the fine mode aerosol, factors were in fact orthogonal since the factor correlation matrix did not show any interrelationship between the factors. On the other hand, the OBLIMIN rotated factors on the coarse mode aerosol data showed that soil related elements were common for two factors. The factor correlation coefficient for these factors was 0.48. However, no significant improvements in the source identification were observed and the original VARIMAX rotated solution was kept for the quantitative analysis of the data.

The total mass source apportionment based on the APFA source profiles revealed that *ca* 49% of the fine suspended particulate matter appeared related to sulfate particles, while 26, 13, 6.4 and 5.6% corresponded to composite wood-burning/automotive emissions, oil combustion, soil dust/metallurgical, and soil dust/wood-burning, respectively. The source apportionment results for the coarse fraction indicate that soil dust is accounted for about 74% of the coarse mode mass concentration, whereas the remaining factors accounted for: 12.8% (composite soil dust/industrial), 9% (SO_4^{2-} composite), 4% (composite soil dust/automotive emissions), and 0.02% (secondary SO_4^{2-} particles).

EPMA measurements allowed the identification of eight different particle types in both fine and coarse mode aerosols, pertaining to soil dust, marine aerosol, gypsum, metallurgical emissions and biomass burning release. This analytical technique provided a better resolution of the different sources affecting the monitoring site than did receptor models. Nevertheless, there is a satisfactory agreement between the results obtained based on the bulk elemental concentrations and those from EPMA regarding source composition and particle size. Thus the most abundant particle type (soil dust) had an average diameter pertaining to the coarse fraction in which, according to receptor models, it represents the most significant source contribution to coarse particle mass concentration. Particles associated with anthropogenic activities (secondary sulfates, metallurgical and wood-burning releases) had diameters corresponding to the fine fraction in which they account for most of the fine particle mass concentration. In the fine fraction S particles did not explicitly appear as an independent group of particles, probably due to the fact that S-bearing particles had diameters below the minimum detectable particle size of 0.26 μm; however, it was present in six out of eight different particle type classifications, which constitutes by itself an evidence of the abundance of this element.

LAMMA results confirmed those previously obtained by EPMA concerning the presence of seaspray in the city of Santiago de Chile airshed. In fact, EPMA measurements indicated that the second most important particle type was marine aerosol, having sub-μm diameters. On the other hand, the positive ion mode spectrum of particles with diameters ranging from 0.25 to 0.5 μm contained a relatively high proportion of transformed seasalt particles, showing S enrichment.

The negative ion mode spectrum was mainly characterized by SO_4^{2-}. The presence of the carbon clusters in the negative mode suggests the impact of fossil-fuel combustion release, which was not detected by the previous analytical techniques. The results regarding marine impact were rather unexpected.

In general, the results provided by three different analytical techniques in addition to those from receptor models, give a broad overview on the air pollution at this location in Santiago de Chile. However, due to the extension of the urban area, future research will require the use of a network of monitoring stations and much longer sampling periods in order to measure, assess and provide the regulatory agency with modern and effective air pollution control strategies.

Acknowledgements—We thank M. E. Cantillano, H. Nuñez, F. Vivanco and J. Jiménez, for their important collaboration during the sampling program. The help provided by L. Kolaitis with LAMMA is gratefully acknowledged. We thank one anonymous reviewer for his useful comments. One of the authors (CMR) is grateful to the International Atomic Energy Agency for a research fellowship. One (PA) is grateful to Fundação de Amparo á Pesquisa do Estado de São Paulo, grant 85/3566-B. Part of this work has been financially supported by the Belgian Ministry of Science Policy under grant 84-89/69.

REFERENCES

Alpert D. J. and Hopke P. K. (1980) A quantitative determination of sources in the Boston urban aerosol. *Atmospheric Environment* **14,** 1137–1146.

Alpert D. J. and Hopke P. K. (1981) A determination of the sources of airborne particles collected during the regional air pollution study. *Atmospheric Environment* **15,** 675–687.

Anderberg M. R. (1973) *Cluster Analysis for Applications.* Academic Press, New York.

Andreae M. O., Charlson R. J., Bruynseels F., Storms H., Van Grieken R. E. and Maenhaut W. (1986) Internal mixture of seasalt, silicates and excess sulfate in marine aerosols. *Science* **232,** 1620.

Artaxo P., Storms H., Bruynseels F., Van Grieken R. and Maenhaut W. (1988) Composition and sources of aerosols from the Amazon Basin. *J. geophys. Res.* **93 (D2),** 1605–1615.

Bauman S., Houmere P. D. and Nelson J. W. (1981) Cascade impactor aerosol samples for PIXE and PESA analysis. *Nuclear Inst. Methods* **181,** 499–502.

Clegg S. L., and Brimblecombe P. (1985) Potential degassing of hydrogen choride from acidified sodium chloride droplets. *Atmospheric Environment* **19,** 465–470.

Cooper J. A. and Watson J. G. (1980) Receptor oriented methods of air particulate source apportionment. *J. Air Pollut. Control Ass.* **30,** 1116–1125.

Denoyer E., Van Grieken R., Adams F. and Natusch D. F. S. (1982) Laser microprobe mass spectrometry 1: basic principles and performance characteristics. *Analyt. Chem.* **54,** 26A.

Dzubay T. G. and Nelson R. O. (1975) Self absorption corrections for x-ray fluorescence analysis of aerosols. *Adv. X-ray Anal.* **18,** 619–631.

Dzubay T. G. and Stevens R. K. (1984) Interlaboratory comparison of receptor models results for Houston aerosol. *Atmospheric Environment* **18,** 1555–1566.

Goldstein J. I., Newbury D. E., Echlin P., Joy D. C., Fiori Ch. and Lifshin E. (1981) *Scanning Electron Microscopy and X-Ray Microanalysis.* Plenum Press, New York.

Gorsuch R. L. (1983) *Factor Analysis.* Lawrence Erlbaum Ass. Publishers, Hillsdale, New Jersey.

Harrison R. M. and Sturges W. T. (1983) The measurements and interpretations of Br/Pb ratios in airborne particles. *Atmospheric Environment* **17,** 311–328.

Heidam N. Z. (1982) Atmospheric aerosol factor models, mass and missing data. *Atmospheric Environment* **16,** 1923–1931.

Heinrich K. F. J. (1981) *Electron Beam X-Ray Microanalysis.* Van Nostrand Reinhold, New York.

Henry R. C., Lewis C., Hopke P. and Williamson H. (1984) Review of receptor models fundamental. *Atmospheric Environment* **18,** 1507–1515.

Hopke P. K., Gladney E. S., Gordon G. E., Zoller W. H. and Jones A. G. (1976) The use of multivariate analysis to identify sources of selected elements in the Boston urban aerosol. *Atmospheric Environment* **14,** 1015–1025.

Mason B. (1966) *Principles of Geochemistry.* Wiley, New York.

Öblad M. and Selin E. (1985) Measurements of Br/Pb ratios in airborne particles from car exhaust. *Physica Scripta* **32,** 462–468.

Parker R. D., Buzzard G. H., Dzubay T. G. and Bell J. P. (1977) A two-stage respirable aerosol sampler using Nuclepore filters in series. *Atmospheric Environment* **11,** 617–621.

Préndez M., Ortiz J. L., Cortés E. and Cassorla V. (1984) Elemental composition of airborne particulate matter from Santiago City, Chile, 1976. *J. Air Pollut. Control Ass.* **34,** 54–56.

Rahn K. A. (1976) The chemical composition of the atmospheric aerosol. Technical Report of the Graduate School of Oceanography, Univ. of Rhode Island, Kingston RI, U.S.A.

Rancitelli L. A., Cooper J. A. and Perkins R. W. (1977) Multielements characterization of atmospheric aerosols by neutron activation analysis and x-ray fluorescence analysis. Proceedings of the Symposium on Comparative Studies on Food and Environmental Contamination. International Atomic Energy Agency, Vienna, Austria.

Receptor Model Source Composition Library (1984) U.S. Environmental Protection Agency. EPA-450/4-85-002.

Rummel R. J. (1970) *Applied Factor Analysis.* Northwestern University Press, Evanston.

Schütz L. and Rahn K. (1982) Trace element concentration in erodible soil. *Atmospheric Environment* **16,** 171–176.

Silo C. and Lissi E. (1982) Suspended matter in the urban air of Santiago. *Proceedings Fifth International Clean Air Conference Buenos Aires, Argentina.*

Stevens R. K. and Thompson G. P. (1984) Overview of the mathematical and empirical receptor models workshop (Quail Roost II). *Atmospheric Environment* **18,** 1499–1506.

Storms H., Artaxo P. Bruynseels F. and Van Grieken R. (1987) Individual particle analysis by automated EPMA for the improvement of source apportionment studies for remote aerosols. In *Microbeam Analysis,* pp. 343–345. San Francisco Press, San Francisco.

Storms H. (1988) Quantification of automated electron microprobe x-ray analysis and application in aerosol research. Ph.D. dissertation, University of Antwerp (UIA).

Thurston G. D. and Spengler J. D. (1985) A quantitative assesment of source contributions to inhalable particulate matter pollution in metropolitan Boston. *Atmospheric Environment* **19,** 9–25.

Trier A. (1984) Observations on inhalable atmospheric particulates in Santiago, Chile. *J. Aerosol Sci.* **15,** 419–421.

Trier A. and Silva C. (1987) Inhalable urban atmospheric particulate matter in a semi-arid climate: the case of Santiago de Chile. *Atmospheric Environment* **21,** 977–983.

Tuncel S. G., Olmez I., Parrington J. R., Gordon G. E. and Stevens R. K. (1985) Composition of fine particle regional

sulfate component in Shenandoah Valley. *Envir. Sci. Technol.* **19,** 529–537.

Van Espen P., Janssens K. and Nobels J. (1986) Axil-PC, Software for the analysis of complex X-ray spectra. *Chemometrics Intelligent Lab. Syst.* **1,** 109–114.

Van Espen P. (1984) A program for the processing of analytical data (DPP). *Anal. Chim. Acta* **165,** 31.

Vogt H., Heinen H. J., Meier S. and Wechsung R. (1981) *Fres. Z. Anal. Chem.* **308,** 195.

Ward J. H. (1963) *J. Am. Stat. Ass.* 58–236.